Development 126, 4499-4511 (1999)
Printed in Great Britain © The Company of Biologists Limited 1999
DEV4221

HNF3β and *Lim1* interact in the visceral endoderm to regulate primitive streak formation and anterior-posterior polarity in the mouse embryo

Aitana Perea-Gómez[1], William Shawlot[2,*], Hiroshi Sasaki[3], Richard R. Behringer[2] and Siew-Lan Ang[1,‡]

[1]Institut de Génétique et de Biologie Moléculaire et Cellulaire, CNRS/INSERM/Université Louis Pasteur, BP163, 67404 Illkirch cedex, CU de Strasbourg, France
[2]Department of Molecular Genetics, The University of Texas M. D. Anderson Cancer Center, Houston, Texas 77030, USA
[3]Laboratory of Developmental Biology, Institute for Molecular and Cellular Biology, Osaka University, Osaka 565, Japan
*Present address: Department of Genetics, Cell Biology and Development, University of Minnesota, Minneapolis 55455, USA
‡Author for correspondence (e-mail: siew-lan@igbmc.u-strasbg.fr)

Accepted 2 August; published on WWW 27 September 1999

SUMMARY

Recent embryological and genetic experiments have suggested that the anterior visceral endoderm and the anterior primitive streak of the early mouse gastrula function as head- and trunk-organising centers, respectively. Here, we report that *HNF3β* and *Lim1* are coexpressed in both organising centers suggesting synergistic roles of these genes in regulating organiser functions and hence axis development in the mouse embryo. To investigate this possibility, we generated compound *HNF3β* and *Lim1* mutant embryos. An enlarged primitive streak and a lack of axis formation were observed in *HNF3β*$^{-/-}$;*Lim1*$^{-/-}$, but not in single homozygous mutant embryos. Chimera experiments indicate that the primary defect in these double homozygous mutants is due to loss of activity of *HNF3β* and *Lim1* in the visceral endoderm. Altogether, these data provide evidence that these genes function synergistically to regulate organiser activity of the anterior visceral endoderm. Moreover, *HNF3β*$^{-/-}$;*Lim1*$^{-/-}$ mutant embryos also exhibit defects in mesoderm patterning that are likely due to lack of specification of anterior primitive streak cells.

Key words: *HNF3β*, *Lim1*, Anteroposterior axis, Mesoderm, Patterning, Visceral endoderm

INTRODUCTION

One of the major questions that arises when studying development of the mouse embryo is the understanding of the mechanisms that allow generation of anteroposterior (A-P) polarity. Indeed after implantation, the mouse embryo is a symmetrical cup-shaped structure consisting of an outer layer of visceral endoderm (VE) and an inner layer of ectoderm. The first morphological sign of asymmetry is the thickening of the embryonic ectoderm, or epiblast, at the junction with the extraembryonic ectoderm in the future posterior region of the embryo. This feature marks the appearance of the primitive streak, where mesoderm is produced by delamination of epiblast cells (Tam and Behringer, 1997, for a review).

Embryological manipulations have shown that the anterior region of the primitive streak and its later derivative, the node, can induce the formation of an anteriorly truncated secondary axis when grafted ectopically in lateral regions of the embryo (Beddington, 1994). Thus, the anterior primitive streak was thought to be the mouse equivalent of the vertebrate gastrula organiser, first defined by Spemann and Mangold in the newt embryo, and subsequently found in all vertebrate species examined (reviewed by Lemaire and Kodjabachian, 1996). Recent genetic and embryological data suggest, however, that an extraembryonic tissue of the mouse gastrula, the anterior visceral endoderm (AVE), displays organising properties as it is necessary to induce and pattern the anterior regions of the mouse embryo (reviewed in Beddington and Robertson, 1998). Indeed ablation experiments have demonstrated a requirement of the AVE for the correct expression of forebrain markers (Thomas and Beddington, 1996). Moreover, chimera analysis has shown that the VE expression of several genes coding for secreted molecules (Nodal) or transcription factors (Otx2 and HNF3β), is essential for head development (Varlet et al., 1997; Rhinn et al., 1998; Dufort et al., 1998). These findings have led to the proposal that the AVE of the mouse embryo displays head organising properties whereas the anterior primitive streak can induce trunk structures. Remarkably, several genes conserved through evolution and expressed in the organiser of different vertebrate embryos are found both in the AVE and in the anterior primitive streak of the mouse gastrula, further confirming that both tissues contribute to organiser function. These genes code for secreted molecules such as Nodal (Varlet et al., 1997) or for transcription factors like the homeodomain proteins Otx2 and Goosecoid (Gsc), the winged helix factor HNF3β and the LIM homeodomain protein Lim1 (Ang and Rossant, 1994; Filosa et al., 1997; Barnes et al., 1994, Shawlot and Behringer, 1995). In addition, Gsc, Lim1, the

homeodomain protein Hex (Thomas et al., 1998) and the secreted molecule Cerberus-like (Cer-l) (Belo et al., 1997) are specifically expressed in the AVE before the appearance of the primitive streak in the posterior side of the embryo, suggesting that the head organiser arises independently of the trunk organiser and that anterior regions are defined before posterior regions of the mouse embryo.

Among the genes expressed in both the AVE and the anterior primitive streak of the mouse embryo, those that code for transcription factors are likely to play a role in specifying the organising properties of these tissues. The in vivo function of these genes has been addressed by gene targeting experiments. *Otx2* has been shown to function in the VE for the induction of forebrain and midbrain (Rhinn et al., 1998, reviewed in Simeone, 1998). Although *Gsc* null mutants are not affected during early development (Rivera-Perez et al., 1995; Yamada et al., 1995), analysis of *Gsc*$^{-/-}$;*HNF3β*$^{+/-}$ compound mutant embryos has demonstrated that *Gsc* functions synergistically with *HNF3β* to pattern the neural tube. The expression patterns of these two genes in early mouse embryos suggest that the interaction could take place during gastrulation either in the anterior primitive streak or in the AVE (Filosa et al., 1997). *HNF3β* mutant embryos show severe defects in dorsoventral (D-V) patterning of the neural tube due to the loss of an organised node and axial mesoderm structures, while the A-P axis is correctly specified in most cases (Ang and Rossant, 1994; Weinstein et al., 1994). However, a role for *HNF3β* in the VE for the development of anterior neural tissue has been inferred from chimera analysis (Dufort et al., 1998). *Lim1* homozygous mutant embryos show a truncation of the neural tube rostral to rhombomere 3, which is due to a defect in AVE and prechordal mesoderm (Shawlot and Behringer, 1995; W. S. and R. R. B., unpublished results). Taken together, these results suggest that the mutation of only one of the transcription factors expressed in the organising centers of the mouse gastrula does not completely impair axis development. These factors might therefore act redundantly or synergistically in the anterior primitive streak and the AVE, as already demonstrated in the case of *Gsc* and *HNF3β* (Filosa et al., 1997).

In this paper, we have investigated the possible interactions and/or redundant functions of *HNF3β* and *Lim1*. A comparative analysis of the expression domains of the two genes has shown that they are coexpressed in the VE layer surrounding the epiblast before primitive streak formation. During gastrulation, a subpopulation of cells in the anterior primitive streak coexpresses the two genes. In the VE, *Lim1* expression is maintained at strong levels only in anterior regions, where it is coexpressed with *HNF3β*. Their early coexpression in organising centers of the mouse gastrula prompted us to generate compound mutant embryos. *HNF3β*$^{-/-}$;*Lim1*$^{-/-}$ mutant embryos show severe germ layer disorganisation and a lack of embryonic ectoderm derivatives. Epiblast development is impaired as early as 6.5 days post-coitum (d.p.c.) as we observe an expansion of the primitive streak territory and a loss of anterior and distal regions. Chimera analysis shows that the primary defect in *HNF3β*$^{-/-}$;*Lim1*$^{-/-}$ mutant embryos lies in the VE. Based on this result and on the analysis of molecular markers of the VE in double mutant embryos, we propose a model for the function of *HNF3β* and *Lim1* in the VE in restricting primitive streak formation to posterior regions of the epiblast, thereby establishing A-P polarity in the mouse embryo. In addition, double mutant embryos also show D-V patterning defects in mesoderm formation that are likely due to an additional function of the two genes in the specification of anterior primitive streak cells.

MATERIALS AND METHODS

Generation and genotyping of wild-type and mutant mice

Lim1 heterozygous mutant mice on a 129/Sv×CD1 background (Shawlot and Behringer, 1995) were crossed with *HNF3β* heterozygous mutant mice on a 129/Sv×CD1 background (Ang and Rossant, 1994) to generate double heterozygous animals. For the genotyping of pups, DNA was extracted from tail tips as described in Laird et al. (1991). For genotyping of 7.5 d.p.c. or older embryos, yolk sac DNA extraction was performed according to Moens et al. (1992). For 6.5 d.p.c. embryos, DNA was extracted from ectoplacental cone cultures as described (Ang and Rossant, 1994). PCR analysis of the *Lim1* locus was performed using the same primers as in Shawlot and Behringer (1995). The DNA was amplified for 35 cycles (94°C/1minute, 55°C/30 seconds, 72°C/1 minute) in 25 μl volume containing 67 mM Tris-HCl, pH 8.8, 6.7 mM $MgCl_2$, 170 μg/ml BSA, 16.6 mM $(NH_4)_2SO_4$, 1.5 mM dNTPs, 10% DMSO and 150 ng of each oligonucleotide. For the *HNF3β* locus, PCR analysis was performed using primers and conditions described in Filosa et al. (1997). Staging of mutant and wild-type embryos was according to Downs and Davies (1993).

In situ hybridisation, immunohistochemistry and histology

Whole-mount in situ hybridisation was performed as described previously (Conlon and Herrmann, 1993). The number of specimens used for in situ hybridisation of each gene is indicated in the figure legends as *n*=X. For section in situ hybridisation, deciduae were fixed for 2 hours in 4% paraformaldehyde in PBS, equilibrated in 20% sucrose and embedded in OCT (Tissue-Tek, Miles). In situ hybridisation on sections was performed as described in Gradwohl et al. (1996), and sections were counterstained with hematoxylin. The following probes were used: *Lim1* (Barnes et al., 1994), *Oct4* (Rosner et al., 1990), *Sox1* (Collignon et al., 1996), *Otx2* (Ang et al., 1994), *T* (Wilkinson et al., 1990), *Fgf8* (Crossley and Martin, 1995), *MesP1* (Saga et al., 1996), *Lefty2* (Meno et al., 1996), *Gsc* (Filosa et al., 1997), *Cer-l* (Belo et al., 1997), *Hex* (Thomas et al., 1998), *Lefty1* (Oulad-Abdelghani et al., 1998), *Pem* (Lin et al., 1994), *Twist* (Wolf et al., 1991), *Delta1* (Bettenhausen et al., 1995), *Tbx6* (Chapman et al., 1996), *Bmp4* (Winnier et al., 1995), *Flk1* (Yamaguchi et al., 1993) and *Fgf3* (Wilkinson et al., 1989).

Whole-mount immunohistochemistry was performed according to published procedures (Davis et al., 1991) using a rabbit polyclonal anti-HNF3β antibody (Filosa et al., 1997) at a dilution of 1:500.

For histological analysis, embryos were fixed overnight in Bouin's fixative, dehydrated and embedded in wax. 7 μm sections were counterstained with Hematoxylin and Eosin (1%), or Safranin-O (0.01%) for embryos previously processed for whole-mount in situ hybridisation, immunohistochemistry or β-galactosidase staining.

Generation and analysis of chimeras

The morulae stage (2.5 d.p.c.) embryos used to generate chimeras were obtained from crosses of double heterozygous *Lim1*$^{+/-}$;*HNF3β*$^{+/-}$ animals. Embryos were injected with approximately 10 wild-type ROSA26/+ ES cells of the ES31 line (Rhinn et al., 1998) and reimplanted into pseudogestant females. Chimeric embryos were harvested at 7.5 d.p.c. and processed for β-galactosidase staining as described in Beddington et al. (1989). The genotype of the host morula was determined retrospectively using visceral yolk sac

endoderm isolated from visceral mesoderm after digestion in pancreatin and trypsin as described (Hogan et al., 1994). DNA samples prepared from the endodermal fraction were genotyped for the *Lim1* and *HNF3β* loci by PCR.

RESULTS

Expression of *Lim1* and *HNF3β* in early mouse embryos

Earlier studies have shown that *Lim1* and *HNF3β* are expressed in the anterior primitive streak as well as in the AVE (Barnes et al., 1994; Shawlot et al., 1995; Filosa et al., 1997). To more precisely compare the expression domains of *HNF3β* and *Lim1*, we analysed the expression of these two genes from pregastrulation to the headfold stage (5.5-7.75 d.p.c.), by radioactive in situ hybridisation on adjacent sections and by double-labelling analyses of embryos in whole mounts. Sagittal sections of 5.5 d.p.c. embryos show expression of both *Lim1* and *HNF3β* in the VE (Fig. 1A-C). *HNF3β* is expressed in the VE lining both the embryonic and extraembryonic regions, whereas *Lim1* expression is found exclusively in the VE in contact with the epiblast. At the onset of gastrulation (6.5 d.p.c.), both transcripts are detected in the newly formed primitive streak at the posterior proximal region of the embryo, and *HNF3β* is still expressed in the whole endoderm germ layer (Fig. 1D,F). In contrast, *Lim1* transcripts can no longer be detected in the region of the VE overlying the primitive streak (arrow in Fig. 1E). As gastrulation proceeds and the primitive streak elongates, *Lim1* transcripts are progressively restricted to the AVE and are also observed in the mesoderm wings (Fig. 1E and data not shown).

Double-labelling by in situ hybridisation with a *Lim1* RNA probe and immunocytochemistry with a HNF3β antiserum on whole embryos at 6.5 d.p.c. demonstrated that HNF3β and *Lim1* are coexpressed in the AVE and in the anterior primitive streak (Fig. 1G,H,J,K). However, in the anterior primitive streak, the majority of the cells and specifically the more distal ones express only HNF3β (Fig. 1H). Thus as we had previously shown for *Gsc* (Filosa et al., 1997), *Lim1* expression is encompassed by the domain of expression of HNF3β in the anterior primitive streak. The mesoderm cells exiting the primitive streak express *Lim1* and HNF3β, whereas the endoderm cells overlying the anterior primitive streak express HNF3β alone (data not shown). In the anterior mesoderm wings only *Lim1* is expressed (Fig. 1K). By the early headfold stage (7.5 d.p.c.) when the primitive streak has reached the distal tip of the embryo and the node and head process are formed, both HNF3β and *Lim1* are expressed in these structures (Fig. 1I). Flatmounts of the distal region of the embryo show a large number of cells coexpressing HNF3β and *Lim1* in the node and in the head process (Fig. 1L). However, *Lim1* expression in the head process seems to be transient as in late head fold stage embryos (7.75 d.p.c.) only HNF3β protein is detected in anterior midline tissues (data not shown). In summary, our results demonstrate that *Lim1* and *HNF3β* are coexpressed in the VE surrounding the epiblast before gastrulation and in a population of cells in the anterior primitive streak and its derivatives (the node and axial mesoderm cells) during gastrulation.

Table 1. Frequencies of genotypes among embryos with mutant phenotype

Genotype		Frequency (%)			
HNF-3β	*Lim-1*	Predicted	6.5 d.p.c. (*n*=70)	7.5 d.p.c. (*n*=62)	8.75 d.p.c. (*n*=64)
–/–	+/+	6.25	8.57	9.67	6.25
–/–	+/–	12.50	10.00	9.67	12.50
+/+	–/–	6.25	8.57	4.83	4.68
+/–	–/–	12.50	11.42	11.29	6.25
–/–	–/–	6.25	2.85	4.83	0

n, Number of embryos analysed.
The fit to mendelian expectations was tested with a χ^2 goodness-of-fit test:
6.5 d.p.c.: χ^2=3.49, df=5, 0.9>*P*>0.5
7.5 d.p.c.: χ^2=3.25, df=5, 0.9>*P*>0.5.

Early lethality of *HNF3β*$^{-/-}$;*Lim1*$^{-/-}$ double mutants

The identification of domains of coexpression of *HNF3β* and *Lim1* raised the possibility that these genes interact in cells of the VE and of the anterior primitive streak. To study genetic interactions between these genes during development, we have generated double heterozygous animals. These mice appeared normal and fertile and when intercrossed gave rise to mutant embryos of five different genotypes at the expected Mendelian frequencies at 6.5 d.p.c. and 7.5 d.p.c. (Table 1). However, from 8.75 d.p.c. onwards, embryos of the *HNF3β*$^{-/-}$;*Lim1*$^{-/-}$ genotype were not recovered, suggesting that these embryos die between 7.5 and 8.75 d.p.c. Thus, *HNF3β*$^{-/-}$;*Lim1*$^{-/-}$ double mutant embryos (referred to as *HNF3β,Lim1* embryos) die 2 days earlier than single *HNF3β*$^{-/-}$ or *Lim1*$^{-/-}$ mutants (Ang and Rossant, 1994; Shawlot et al., 1995; Weinstein et al., 1994). In contrast, embryos of the genotypes *HNF3β*$^{-/-}$;*Lim1*$^{+/-}$ and *HNF3β*$^{+/-}$;*Lim1*$^{-/-}$ were found at the expected Mendelian ratios at 10.5-11.5 d.p.c., indicating that these embryos do not die earlier than single mutants (data not shown).

HNF3β,Lim1 embryos show severe germ layer disorganisation

The earlier lethality of *HNF3β,Lim1* embryos suggested that these mutants are more severely affected than the single homozygous mutants. This result was confirmed by morphological and histological analysis. *HNF3β,Lim1* embryos are easily recognizable morphologically from their littermates as early as 6.75 d.p.c. by the compact appearance of their embryonic region (Fig. 2A-D and data not shown). In wild-type embryos, the cavitation process is over at this stage and has produced a central lumen called the amniotic cavity, resulting in their characteristic cup-shaped appearance (Fig. 2A). In contrast, the amniotic cavity is absent or very small in *HNF3β,Lim1* embryos (Figs 2D, 3B). Single mutant embryos show a central cavity despite their abnormal shape and characteristic constriction at the embryonic-extraembryonic junction (Fig. 2B,C).

Sagittal sections through a *HNF3β,Lim1* embryo at 6.75 d.p.c. show that the epiblast (which normally gives rise to the embryonic tissues upon gastrulation) is disorganised (Fig. 3B) and lacks the typical columnar aspect observed in a wild-type littermate (Fig. 3A). The extraembryonic ectoderm is prematurely detached from the embryonic ectoderm (asterisk

in Fig. 3B) but other extraembryonic structures, including proximal and distal VE, look normal. The space between embryonic and extraembryonic ectoderm is filled with cells of a mesenchymal appearance. It is to note that none of the embryos of the other genotypes showed such phenotypic features (data not shown).

At 7.75 d.p.c., *HNF3β,Lim1* embryos have a very small embryonic region (Fig. 2H) when compared to wild-type (Fig. 2E) or single mutant embryos (Fig. 2F,G), whereas the extraembryonic region looks normal in size. Unlike in the wild-type embryos at this stage (Fig. 3C), we could not distinguish the three germ layers in the embryonic region of *HNF3β,Lim1* embryos. Neither a continuous mesoderm layer nor neurectodermal folds are visible. Instead, the embryonic region of these embryos is severely disorganised and presents multiple cavities (Fig. 3D), whereas the extraembryonic region and the outer VE layer seem to be correctly formed. In these embryos, it is also possible to identify some extraembryonic mesoderm lining the chorion and the proximal VE (arrowhead in Fig. 3D).

Thus, *HNF3β,Lim1* embryos show a new and more severe phenotype than the single *HNF3β*$^{-/-}$ and *Lim1*$^{-/-}$ mutant embryos. The organisation of the germ layers is strongly impaired in the embryonic region, presumably as a consequence of the disorganisation of the epiblast at earlier stages. However, gastrulation has occurred as mesoderm is produced in these embryos.

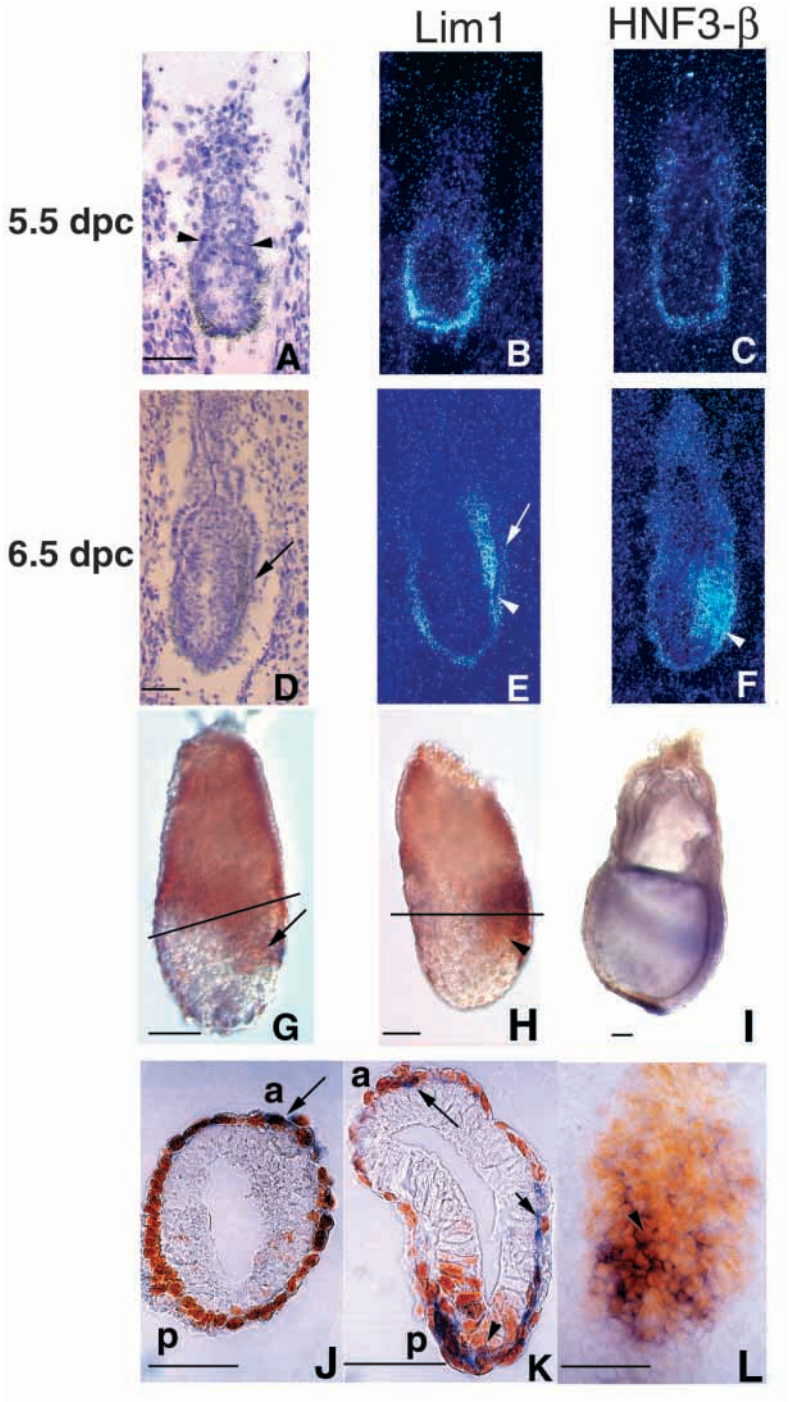

Absence of embryonic ectoderm derivatives in *HNF3β,Lim1* mutants

At 7.75 d.p.c., the ectoderm of a wild-type embryo consists of an epithelial layer that was never observed in *HNF3β,Lim1* embryos (Fig. 3C,D). To further characterise the defects in the ectodermal layer of *HNF3β,Lim1* embryos, we analysed the expression of *Oct4* and *Sox1* in these embryos. *Oct4* belongs to the family of POU domain transcription factors and is expressed at 7.5 d.p.c. in definitive ectoderm in the posterior half as well as in the primitive streak (Fig. 4A; Rosner et al., 1990). However in *HNF3β,Lim1*

Fig. 1. *Lim1* and *HNF3β* are coexpressed in the VE, anterior primitive streak and its derivatives in early mouse embryos. (A-F) Radioactive in situ hybridisation on adjacent sagittal sections. (A,D) Bright-field images of sections shown in B and E, respectively. Arrowheads in A point to the embryonic-extraembryonic junction, while the arrow in D points to the VE overlying primitive streak. (B,C) At 5.5 d.p.c., *Lim1* transcripts are found in the VE lining the epiblast with apparently stronger levels in the distal region, while *HNF3β* is expressed in the VE lining the embryonic and extraembryonic regions. (E) At 6.5 d.p.c., *Lim1* is still expressed in the VE except in the region overlying the primitive streak (arrow). *Lim1* transcripts are also found in the anterior primitive streak (arrowhead) and in the mesoderm wings. (F) *HNF3β* is still expressed in the whole VE as well as in the anterior primitive streak (arrowhead). (G-L) Whole-mount in situ hybridisation using *Lim1* RNA probe (purple) and immunohistochemistry with anti-HNF3β antibody (brown). The level of the transverse section depicted in J and K is indicated by horizontal black lines in G and H, respectively. (G,J) At 6.25 d.p.c., *Lim1* and HNF3β are coexpressed in the AVE (arrow in J) and in the anterior primitive streak. (arrow in G). (H,K) A 6.5 d.p.c. embryo showing that the most anterior cells of the primitive streak express only HNF3β (arrowhead in H), whereas more posteriorly both HNF3β and *Lim1* are expressed (arrowhead in K).There is also coexpression of HNF3β and *Lim1* in the AVE (arrow in K). In the anterior mesoderm wings, only *Lim1* is expressed (short arrow). (I,L) At 7.5 d.p.c., *Lim1* and HNF3β are expressed in the node and in the head process. (L) Flatmount of the distal region of the embryo depicted in I shows cells coexpressing *Lim1* and HNF3β (arrowhead in L). Anterior is to the left in A-I, and to the top in J-L. Abbreviations: a, anterior; p, posterior. Scale bar, 50 μm.

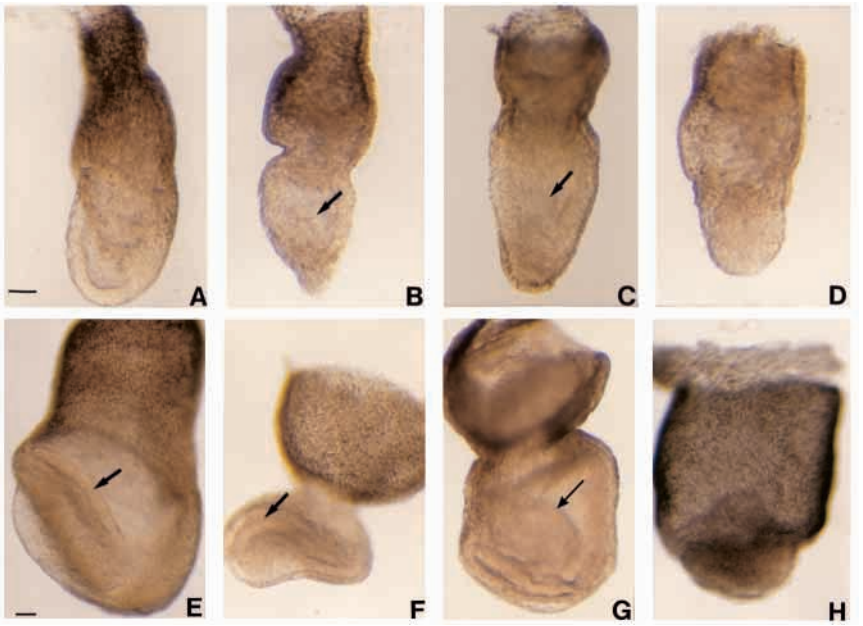

Fig. 2. Mutant phenotypes generated from *HNF3β*$^{+/-}$;*Lim1*$^{+/-}$ intercrosses. (A-D) 6.75 d.p.c. embryos; (E-H) 7.75 d.p.c. embryos. (A) Wild-type embryo. (B) *HNF3β*$^{-/-}$;*Lim1*$^{+/+}$ embryo. (C) *HNF3β*$^{+/+}$;*Lim1*$^{-/-}$ embryo. Both single mutant embryos have a normal amniotic cavity (arrow in B and C). (D) *HNF3β*$^{-/-}$;*Lim1*$^{-/-}$ embryo. The embryonic region is compact and no amniotic cavity is visible. (E) Wild-type embryo. (F) *HNF3β*$^{-/-}$;*Lim1*$^{+/+}$ embryo. (G) *HNF3β*$^{+/+}$;*Lim1*$^{-/-}$ embryo. Wild-type and single mutant embryos have neural folds (arrow in E-G). (H) *HNF3β*$^{-/-}$;*Lim1*$^{-/-}$ embryo. The different germ layers cannot be recognised in the small embryonic region. In contrast, extraembryonic tissues appear normal in size. Extraembryonic is to the top, anterior is to the left. Magnification is the same for A-D and E-H, respectively. Scale bar in A and E, 100 μm.

mutants, *Oct4* transcripts were absent, suggesting that definitive ectoderm cells are missing in these embryos (Fig. 4A′). *Sox1* is an SRY-related factor expressed in newly formed neural tissue (Fig. 4B and Collignon et al., 1996). In *HNF3β,Lim1* embryos at 7.75 d.p.c., *Sox1* expression was not detected (Fig. 4B′) confirming the lack of neurectoderm suggested by the histological analysis. Altogether, these results show that *HNF3β,Lim1* embryos lack embryonic ectoderm cells and their derivatives at late gastrulating stages. In contrast, the extraembryonic ectoderm of the chorion seems to be correctly formed (asterisk in Fig. 3B,D).

To provide insights into the mechanisms leading to the loss of ectoderm cells, we analysed expression of two epiblast markers, *Otx2* and *Oct4*, in *HNF3β,Lim1* embryos at 6.5 d.p.c. The homeobox gene *Otx2* is normally expressed in epiblast cells of wild-type embryos at this stage, except those at the posterior proximal end (Fig. 4C; Ang et al., 1994). In contrast, *Otx2* expression was not detected in *HNF3β,Lim1* embryos (Fig. 4C′), suggesting abnormal specification of these cells. *Oct4* expression, however, was still observed in *HNF3β,Lim1* embryos (Fig. 4D′) at 6.75 d.p.c., albeit at reduced levels compared to wild-type embryos (Fig. 4D). This apparent lower level of expression is reminiscent of the situation in the primitive streak of normal embryos, where *Oct4* appears to be progressively downregulated as *Brachyury (T)* expression is turned on in cells of the primitive streak (Fig. 4D and data not shown). These results suggest that *HNF3β,Lim1* embryos present defects in patterning of epiblast cells along the A-P axis, although these data alone do not exclude the possibility that an earlier block in epiblast differentiation occurs in *HNF3β,Lim1* embryos.

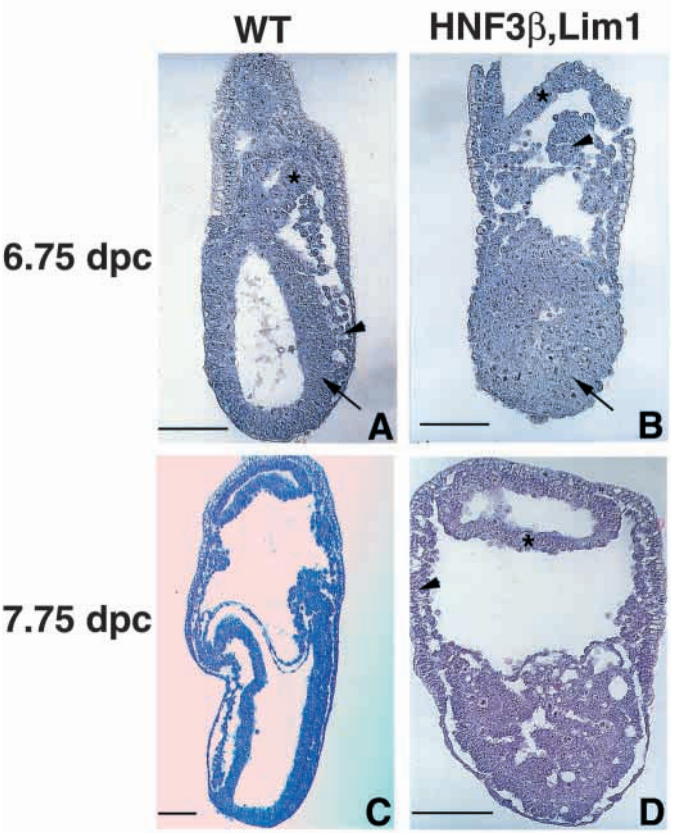

Fig. 3. Histological analysis of *HNF3β,Lim1* embryos. (A,B) Sagittal sections of 6.75 d.p.c. embryos; (C,D) Sagittal sections of 7.75 d.p.c. embryos. (A) Wild-type embryo. The epiblast is a columnar epithelium (arrow) and is still connected to the extraembryonic ectoderm (asterisk). Mesoderm cells are being produced in the posterior region (arrowhead). (B) *HNF3β,Lim1* embryo. The epiblast is disorganised (arrow) and prematurely detached from the extraembryonic ectoderm (asterisk). The extraembryonic region is filled with cells of mesenchymal appearance (arrowhead). (C) Wild-type embryo. Three distinct germ layers can be observed in the embryonic region. (D) *HNF3β,Lim1* embryo. Distinct germ layers cannot be recognised in the embryonic region; however, the extraembryonic mesoderm (arrowhead) and the chorion (asterisk) are correctly formed. Anterior is to the left. Scale bar, 100 μm.

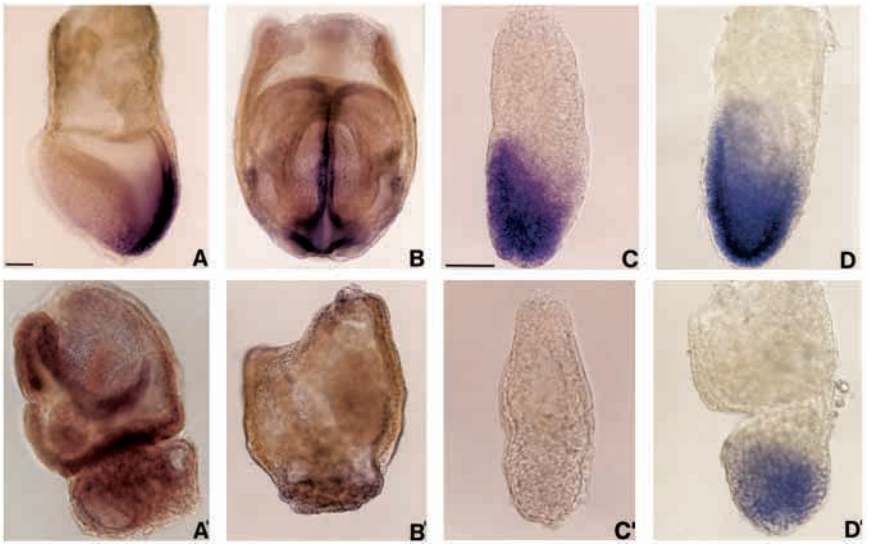

Fig. 4. Absence of embryonic ectoderm derivatives in *HNF3β,Lim1* embryos. Whole-mount in situ hybridisation on wild-type embryos (A-D) and *HNF3β,Lim1* embryos (A′-D′). (A) *Oct4* is expressed in ectoderm cells in the posterior half of wild-type embryos. (A′) Absence of *Oct4* transcripts in a 7.75 d.p.c. *HNF3β,Lim1* embryo (*n*=2). (B) Frontal view of a wild-type embryo showing *Sox1* expression in the neural plate. (B′) Absence of *Sox1* expression in a *HNF3β,Lim1* embryo (*n*=2). (C) *Otx2* is expressed in the anterior two thirds of the epiblast of a wild-type embryo at 6.75 d.p.c. (C′) *Otx2* expression is not detected in a *HNF3β,Lim1* embryo at 6.75 d.p.c. (*n*=2). (D) *Oct4* expression in the epiblast of a wild-type embryo at 6.75 d.p.c. (D′) Reduced levels of *Oct4* expression in the abnormal epiblast of a *HNF3β,Lim1* embryo at 6.75 d.p.c. (*n*=4). Anterior is to the left except in B. Magnification is the same for A,B,A′,B′ and C,D,C′,D′, respectively. Scale bar in A and C, 100 μm.

An enlarged primitive streak territory leads to ectopic mesoderm formation in *HNF3β,Lim1* embryos

We next examined whether the primitive streak develops normally in *HNF3β,Lim1* embryos, by analysing expression of *T* in these embryos. At 6.5 d.p.c., *T* expression is restricted to primitive streak cells in the posterior side of wild-type embryos (Fig. 5A; Wilkinson et al., 1990). In contrast, we observed that *T* transcripts are not restricted to the posterior side in *HNF3β,Lim1* embryos at the same stage (Fig. 5A′), but are present in the whole embryonic region. This result, together with the absence of *Otx2* expression and the low levels of *Oct4* transcripts, strongly suggests that the epiblast of *HNF3β,Lim1* embryos has adopted characteristics of primitive streak cells. This hypothesis is further supported by the expression of *Fgf8* in *HNF3β,Lim1* embryos. During gastrulation, *Fgf8* is expressed in the primitive streak (Fig. 5B; Crossley and Martin, 1995). In *HNF3β,Lim1* embryos, *Fgf8* expression was detected in the entire embryonic region (Fig. 5B′), thus confirming the expansion of the primitive streak territory in these mutants.

The expanded primitive streak domain in *HNF3β,Lim1* embryos suggest that mesoderm might be ectopically produced in these embryos. To examine the extent of mesoderm formation in *HNF3β,Lim1* embryos, we analysed expression of two early markers of mesodermal precursors, *MesP1* and *Lefty2*. The basic helix-loop-helix gene, *MesP1*, is expressed in mesoderm cells as well as in the primitive streak from the

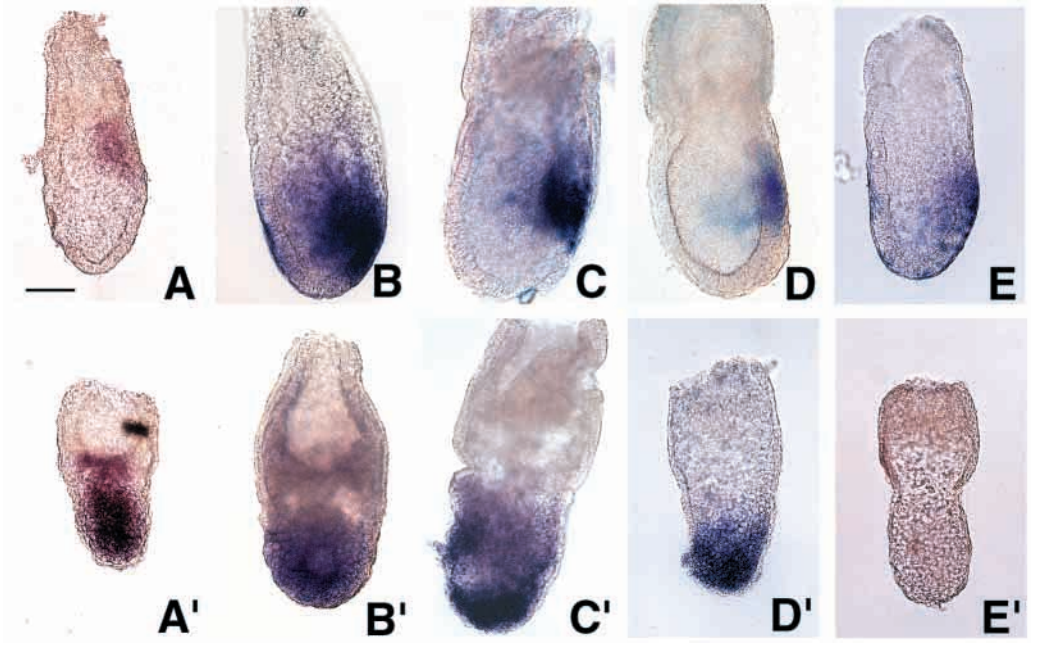

Fig. 5. Enlarged primitive streak region in *HNF3β,Lim1* embryos. Whole-mount in situ hybridisation on 6.5 d.p.c. (A,A′,E,E′) and 6.75 d.p.c. (B-D,B′-D′) wild-type (A-E) and *HNF3β,Lim1* embryos (A′-E′). (A) *T* transcripts are restricted to the posterior region in a wild-type embryo. (A′) *HNF3β,Lim1* embryo showing ectopic *T* expression in the whole embryonic region (*n*=4). (B) *Fgf8* is expressed in the primitive streak of wild-type embryos. (B′) *HNF3β,Lim1* embryo showing *Fgf8* expression in the whole embryonic region (*n*=3). (C) *MesP1* expression in the primitive streak and in the nascent mesoderm cells of a wild-type embryo. (C′) Abundant distal and lateral expression of *MesP1* in a *HNF3β,Lim1* embryo (*n*=1). (D) *Lefty2* is expressed in the middle part of the primitive streak of a wild-type embryo and in mesoderm cells emerging from it. (D′) Widespread expression of *Lefty2* in the whole embryonic region of a *HNF3β,Lim1* embryo (*n*=1). (E) A wild-type embryo showing *Gsc* expression in anterior primitive streak as well as in VE cells. (E′) *Gsc* transcripts are not detected in a *HNF3β,Lim1* embryo (*n*=4). Anterior is to the left. Magnification is the same for all panels. Scale bar in A, 100 μm.

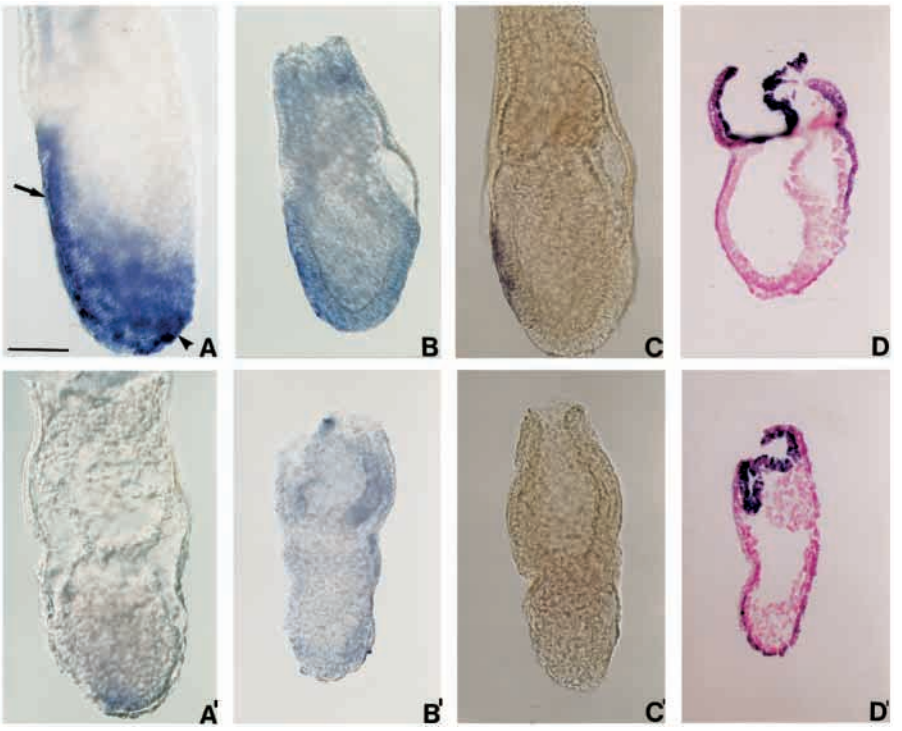

Fig. 6. Abnormal VE in *HNF3β,Lim1* embryos. Whole-mount in situ hybridisation on wild-type (A-D) and *HNF3β,Lim1* (A′-D′) embryos. (A) Cer-l is expressed in the AVE (arrow) and in definitive endoderm cells (arrowhead) of a 6.75 d.p.c. wild-type embryo. (A′) *Cer-l* is expressed faintly in a few distal cells of a *HNF3β,Lim1* embryo (*n*=4). (B) *Hex1* expression in the AVE of a wild-type 6.5 d.p.c. embryo. (C′) *Hex1* expression was not detected in a 6.5 d.p.c. *HNF3β,Lim1* embryo (*n*=2). (C) *Lefty1* is expressed in the AVE of a 6.5 d.p.c. wild-type embryo. (C′) *Lefty1* transcripts are absent in the VE of a *HNF3β,Lim1* embryo (*n*=2). (D) Sagittal section of a 7.5 d.p.c. wild-type embryo showing *Pem* expression in the extraembryonic ectoderm, in the VE in extraembryonic and proximal embryonic region. (D′) Sagittal section of a 7.5 d.p.c. *HNF3β,Lim1* embryo, showing persistent *Pem* expression in VE located ectopically in the distal embryonic region (*n*=2). Anterior is to the left. Magnification is the same for all panels. Scale bar in A, 100 μm.

onset of gastrulation to the late streak stage (Fig. 5C and Saga et al., 1996). In *HNF3β,Lim1* embryos, *MesP1* expression was detected in the distal region as well as in the cells surrounding the small central amniotic cavity of the embryo at 6.75 d.p.c. (Fig. 5C′). Likewise, the TGFβ-family member *Lefty2*, which marks the middle part of the primitive streak as well as the mesoderm cells exiting from it (Fig. 5D; Meno et al., 1996), is expressed in a larger domain including the whole distal embryonic region of *HNF3β,Lim1* embryos (Fig. 5D′). These observations suggest that in *HNF3β,Lim1* embryos mesoderm formation is not confined to posterior regions as in wild-type embryos, but occurs throughout the embryonic region.

Anterior primitive streak cells are missing in *HNF3β,Lim1* embryos

As *HNF3β* and *Lim1* are coexpressed in the anterior primitive streak, we analysed in more detail the status of this structure using the homeobox gene *Gsc*. *Gsc* is expressed in the anterior primitive streak (Fig. 5E; Blum et al., 1992), and its expression has been associated to the presence of organiser cells in several vertebrate species (reviewed by Tam and Behringer, 1997). In single *Lim1* or *HNF3β* mutant embryos, *Gsc* is still expressed but ectopically located in a proximal region of the embryo, presumably due to the lack of elongation of the primitive streak (Shawlot and Behringer, 1995; Ang and Rossant, 1994). At 6.5 d.p.c., *Gsc* expression was

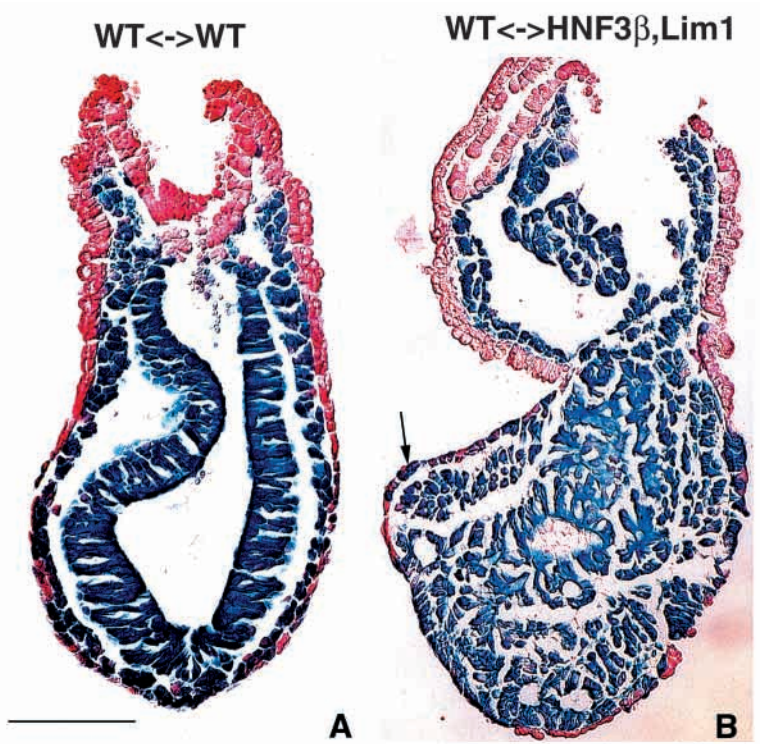

Fig. 7. Lack of rescue of the *HNF3β,Lim1* mutant phenotype by wild-type (WT) embryonic cells in WT↔*HNF3β*$^{-/-}$;*Lim1*$^{-/-}$ chimeric embryos. (A) Sagittal section of a control WT↔WT at 7.5 d.p.c. Wild-type ES cells expressing β-galactosidase have contributed to all the embryonic tissues and to the extraembryonic mesoderm. (B) Sagittal section of a WT↔*HNF3β*$^{-/-}$;*Lim1*$^{-/-}$ chimeric embryo at 7.5 d.p.c. The embryonic region and the extraembryonic mesoderm are exclusively made of wild-type cells, and only the outer VE and the extraembryonic ectoderm are derived from the *HNF3β*$^{-/-}$;*Lim1*$^{-/-}$ morula. The disorganised aspect of the embryonic region indicates that the double mutant phenotype is not rescued, and thus points to a role of *HNF3β* and *Lim1* in the VE. The arrow points to a few wild-type cells with cuboidal morphology in the endoderm layer. Anterior is to the left. Magnification is the same for both panels. Scale bar in A, 100 μm.

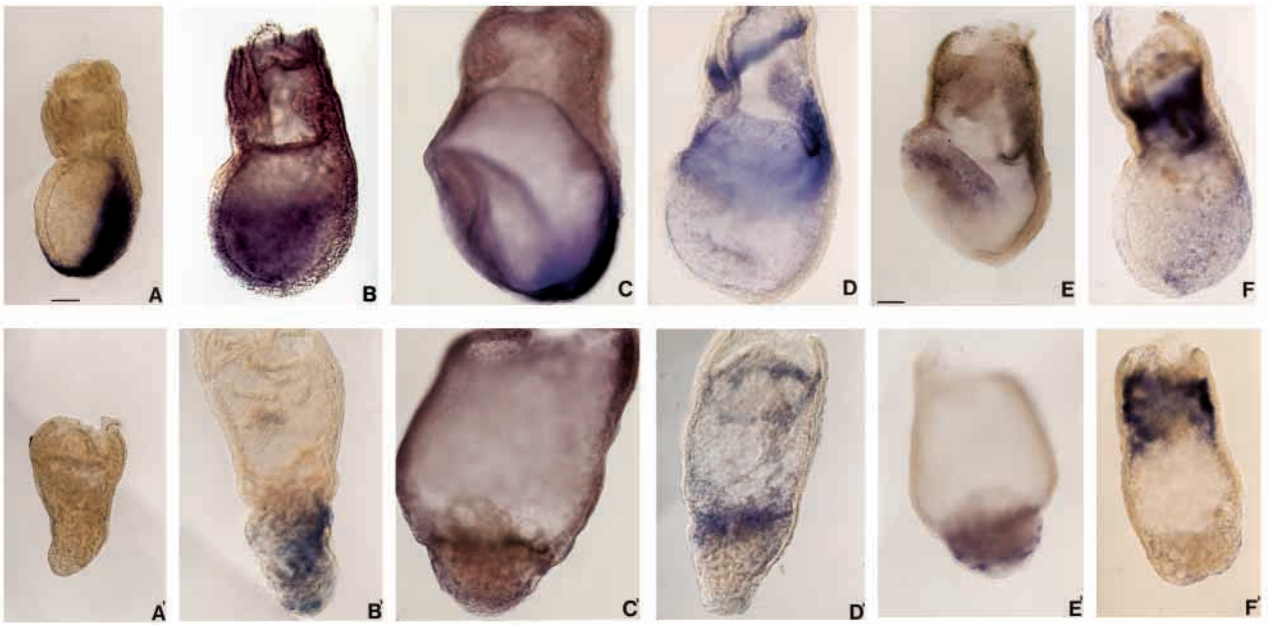

Fig. 8. Absence of dorsal mesoderm in *HNF3β,Lim1* embryos. Whole-mount in situ hybridisation with mesodermal markers on 7.5-7.75 d.p.c. wild-type (A-F) and *HNF3β,Lim1* (A′-F′) embryos.(A) *T* expression in the primitive streak and head process of a wild-type embryo. (A′) *T* expression is absent in a *HNF3β,Lim1* embryo at 7.5 d.p.c., indicating that axial mesoderm is not produced and that primitive streak function has stopped by this stage (*n*=3). (B) Wild-type *Twist* expression in lateral and ventral mesoderm cells. (B′) *Twist* expression in the whole embryonic region of a *HNF3β,Lim1* embryo (*n*=3). (C) *Delta1* is expressed in the paraxial mesoderm and in the primitive streak of a wild-type embryo. (C′) *Delta1* transcripts are not detected in a *HNF3β,Lim1* embryo (*n*=2). (D) *Bmp4* wild-type expression in the ventral mesoderm, in the base of the allantois and in the chorion. (D′) *Bmp4* expression is found normally in the proximal region and in the chorion of a *HNF3β,Lim1* embryo (*n*=1). (E) *Flk1* expression in endothelial precursors located in the proximal region of a wild-type embryo. (E′) Ectopic distal expression of *Flk-1* in a *HNF3β,Lim1* embryo (*n*=2). (F) *Fgf3* expression in extraembryonic mesoderm cells and primitive streak of a wild-type embryo. (F′) In a *HNF3β,Lim1* embryo, *Fgf3* is expressed only in extraembryonic mesoderm cells (*n*=2). Anterior is to the left. Magnification is the same for all panels, except E,E′. Scale bar in A and E, 100 μm.

not detected in *HNF3β,Lim1* embryos, suggesting that the anterior primitive streak and the organiser cells are missing in these mutants (Fig. 5E′). As the anterior primitive streak is the region where the precursors of the axial mesoderm are located, the absence of this structure suggests that there could also be defects in mesoderm patterning in *HNF3β,Lim1* embryos.

Abnormal VE patterning in *HNF3β,Lim1* embryos

Recent findings have revealed a key role of the VE layer in the patterning of the mouse embryo before and during gastrulation (Beddington and Robertson, 1998, 1999). The early disruption in germ layer formation and organisation in *HNF3β,Lim1* embryos, as well as the coexpression of *HNF3β* and *Lim1* in the VE before the onset of gastrulation, prompted us to examine the status of the VE in *HNF3β,Lim1* embryos.

Three genes that are asymmetrically expressed in the VE are *Cer-l, Hex* and *Lefty1*. *Cer-l*, a gene that shares sequence homology with *Xenopus Cerberus* (*X-cer*), encodes a secreted molecule which starts to be expressed in the AVE before the onset of gastrulation and is subsequently found in the definitive endoderm, midline mesoderm and newly formed somites (Fig. 6A and Belo et al., 1997). *Hex* is a homeobox gene expressed first in the distal VE and then asymmetrically in the AVE before primitive streak formation (Fig. 6B; Thomas et al., 1998). Lefty1 is a TGFβ-related molecule, which is expressed specifically in AVE at 6.5 d.p.c. (Oulad-Abdelghani et al., 1998). In *HNF3β,Lim1* embryos, Cer-l, *Hex* and *Lefty1* transcripts are severely reduced or absent in the VE. (Fig. 6A′,B′,C′, respectively). Moreover, *Otx2* and *Gsc*, which normally mark also the AVE, are not expressed in the VE of *HNF3β,Lim1* embryos (Figs 4C′, 5E′, respectively). In contrast, a general marker of VE, *Pem* (Lin et al., 1994), is expressed in *HNF3β,Lim1* embryos at 7.5 d.p.c.; however, expression persists distally in these mutants in contrast to the wild-type situation where *Pem*-positive VE cells have been displaced to proximal regions (Fig. 6D,D′). Thus, although VE is formed in *HNF3β,Lim1* embryos, its molecular patterning seems to be severely impaired, which might be the primary cause of the germ-layer defect in these mutants.

Synergistic functions of *HNF3β* and *Lim1* in the VE

In order to examine specifically the role of *HNF3β* and *Lim1* in the VE, we have generated chimeric embryos by injecting wild-type embryonic stem (ES) cells carrying a ubiquitously expressed *lacZ* transgene into morulae obtained from crosses between double heterozygous mice. In these experiments, one in 16 chimeric embryos would be expected to be derived from a double homozygous mutant morula. This approach takes advantage of the observation that ES cells colonize predominantly the epiblast and the embryonic derivatives in ES cell-morula chimeras. Thus, in a highly chimeric embryo, the extraembryonic ectoderm and the VE are of host origin whereas the epiblast is completely derived from the ES cells (Fig. 7A).

Out of 33 embryos obtained from ES cell-morula

aggregation experiments and analysed at 7.5 d.p.c., 24 were chimeric as revealed by β-galactosidase staining. Of these, two chimeras were derived from injection into *HNF3β*$^{-/-}$*;Lim1*$^{-/-}$ morulae, as determined by PCR-genotyping of yolk-sac endoderm, and looked very similar to *HNF3β,Lim1* embryos. These embryos show an embryonic region that is highly disorganised, formed of cells with a round morphology that do not resemble ectoderm or neurectoderm tissue (Fig. 7B). In contrast, their extraembryonic region is well formed. In these chimeric embryos, only the VE and the extraembryonic ectoderm were *lacZ*-negative (pink cells) and therefore derived from the double mutant morula, whereas the rest of the embryonic and extraembryonic tissues were derived from wild-type ES cells expressing *lacZ* (blue cells). The lack of rescue of the double mutant phenotype despite the high colonisation of the epiblast by wild-type cells, demonstrates that the primary defect in *HNF3β,Lim1* embryos is in VE cells.

It is noteworthy that some *lacZ*+ cells, with a VE-like morphology, are found in the endoderm of the double mutant-derived chimeric embryos (arrow in Fig. 7B), suggesting that the exclusion of the ES cells from the extraembryonic tissues of the chimeras is not complete. One possible explanation for the incomplete exclusion of ES cells from the VE is that the mutant embryo-derived cells in the chimeras are somewhat compromised in their ability to contribute to the VE layer. Alternatively, the *lacZ*+ cells in the *VE* could correspond to gut endoderm cells whose morphology is abnormal as a consequence of defects in the epiblast. Even if the first hypothesis turns out to be the correct one, the presence of a few wild-type cells in the VE of the chimeras is not sufficient to rescue the mutant phenotype, further supporting important roles of *HNF3β* and *Lim1* in the VE.

Mesoderm patterning is affected in *HNF3β,Lim1* embryos

Despite abnormal epiblast and VE development, mesoderm is formed in *HNF3β,Lim1* embryos as shown by the expression of *MesP1* and *Lefty2*. To examine whether different D-V types of mesoderm are produced in double mutant embryos, we determined expression of molecular markers expressed specifically in these different cell types at 7.5-7.75 d.p.c. Using whole-mount in situ hybridisation, we analysed the expression of *T*, a marker of primitive streak and axial mesoderm cells in wild-type embryos at 7.5 d.p.c. (Fig. 8A; Wilkinson et al., 1990). In *HNF3β,Lim1* embryos, *T* expression was not observed, indicating that axial mesoderm is not produced in the mutants (Fig. 8A′). This result is not surprising as *HNF3β*$^{-/-}$ single mutants lack the notochord precursors (Ang and Rossant, 1994; Weinstein et al., 1994) and *Lim1*$^{-/-}$ mutants are devoid of prechordal mesoderm (Shawlot and Behringer, 1995). However, the absence of *T* expression suggests also that the primitive streak has been lost in *HNF3β,Lim1* embryos at 7.5 d.p.c. Thus, mesoderm production is completed by this stage in the double mutants, whereas in the single mutants of the same stage, the primitive streak is still present.

To determine if other types of mesoderm are produced in *HNF3β,Lim1* embryos, we analysed the expression of the bHLH gene *Twist*, a marker of paraxial and lateral ventral mesoderm at 7.5 d.p.c. (Fig. 8B; Wolf et al., 1991). In *HNF3β,Lim1* embryos, *Twist* is widely expressed in the embryonic region, indicating that non-axial mesoderm derivatives are produced in these embryos (Fig. 8B′). To identify specifically paraxial mesoderm cells, a dorsal type of mesoderm that gives rise to the somites later in development, we used two molecular markers specific for this population of mesoderm cells, the Tbox-related gene *Tbx6* and the Notch ligand *Delta1* (Fig. 8C; Chapman et al., 1996; Bettenhausen et al., 1995). At 7.75 d.p.c., neither of these two paraxial mesoderm markers was detected in *HNF3β,Lim1* embryos (Fig. 8C′ and data not shown), whereas the single mutants show expression of both genes (data not shown). Taken together, these results indicate that dorsal mesoderm derivatives (axial and paraxial) are absent in *HNF3β,Lim1* embryos.

In order to analyse the formation of ventral embryonic mesoderm in *HNF3β,Lim1* embryos, we characterised the expression of *Bmp4* and *Flk1*. The TGFβ-related molecule BMP4 is expressed at 7.5 d.p.c. in the ventral mesoderm of the proximal region of the embryo, in the base of the allantois and in the chorion (Fig. 8D; Winnier et al., 1995; Waldrip et al., 1998). In *HNF3β,Lim1* embryos, *Bmp4* transcripts were found in a band at the embryonic-extraembryonic junction indicating the presence of ventral embryonic mesoderm cells in these mutant embryos (Fig. 8D′). In addition, the expression of *Bmp4* in the chorion of *HNF3β,Lim1* embryos confirmed the histological observation that this structure is correctly formed in these mutants. Flk1 is a tyrosine kinase receptor expressed in early endothelial precursors (Fig. 8E; Yamaguchi et al., 1993). In *HNF3β,Lim1* embryos, the expression of *Flk1* was detected not only in the proximal region of the embryo but also in the more distal region (Fig. 8E′). This distal expression suggest that in *HNF3β,Lim1* mutants embryonic ventral mesoderm cells are ectopically located. Altogether these results indicate that ventral embryonic mesoderm cells are formed in *HNF3β,Lim1* embryos.

Finally, we investigated the formation of the most ventral mesoderm derivative, the extraembryonic mesoderm, in *HNF3β,Lim1* embryos. To determine the presence of visceral yolk sac extraembryonic mesoderm, we analysed the expression of the growth factor *Fgf3* (Fig. 8F; Wilkinson et al., 1989). In *HNF3β,Lim1* embryos as well as in the wild-type littermates, *Fgf3* transcripts were found in the extraembryonic region demonstrating that the round cells observed in the extracoelomic cavity of the mutants in histological sections are indeed extraembryonic mesoderm cells (Fig. 8F′). In summary, only ventral mesoderm (embryonic and extraembryonic) is produced in *HNF3β,Lim1* embryos. The dorsal mesoderm derivatives, paraxial and axial mesoderm, are missing indicating that mesoderm patterning is severely impaired in *HNF3β,Lim1* embryos.

DISCUSSION

Abnormal A-P patterning of the epiblast in *HNF3β,Lim1* embryos

The first morphological sign of A-P pattern in the epiblast of the mouse embryo is the site of formation of the primitive streak at the posterior end of the embryo. The genetic pathway that initiates primitive streak formation remains to be elucidated, but expression of *T* on one side of the epiblast at the onset of gastrulation marks posterior primitive streak cells. In *HNF3β,Lim1* embryos, *T* expression in the epiblast is no

longer restricted posteriorly, but is instead expressed throughout the epiblast by the mid-streak stage. Thus, A-P polarity of the epiblast is abnormal in *HNF3β,Lim1* embryos and widespread expression of *T* strongly suggests that mutant epiblast cells are transformed into primitive streak cells. The loss of epiblast cells is confirmed by the absence and reduction of expression of *Otx2* and *Oct4*, respectively. In addition, mid-streak-stage embryos also show ectopic mesoderm formation as demonstrated by the expression of *MesP1* and *Lefty2*. As a consequence of these early patterning defects, ectoderm and neurectoderm cells that are derived from distal and anterior epiblast cells (Lawson et al., 1991) are missing in these embryos at 7.5-7.75 d.p.c. These epiblast defects are not observed in single homozygous *HNF3β* and *Lim1* mutants. Altogether, these data demonstrate that *HNF3β* and *Lim1* function synergistically to establish A-P patterning of the epiblast and to restrict primitive streak formation to the posterior side of mouse embryos.

HNF3β and *Lim1* regulate the patterning function of the VE

A detailed analysis of the expression patterns of *HNF3β* and *Lim1* by in situ hybridization on sections and double-labelling experiments, demonstrates two distinct sites of coexpression. At 5.5 d.p.c., *HNF3β* and *Lim1* are coexpressed in the distal two thirds of the VE. 1 day later, these genes are coexpressed in the AVE and in the anterior primitive streak of mouse embryos. Since the whole epiblast is affected in *HNF3β,Lim1* embryos, it is unlikely that loss of activity of *HNF3β* and *Lim1* in anterior primitive streak cells is the primary cause of the epiblast defects. Rather, the earlier and widespread coexpression of *HNF3β* and *Lim1* in the VE suggests that these two genes are required in this tissue. VE has been shown to regulate growth and cell survival as well as A-P patterning of the early mouse embryo (Beddington and Robertson, 1998). The phenotype of *HNF3β,Lim1* embryos strongly suggests that the patterning function rather than the trophic function of the VE is affected in these mutant embryos. In particular, the finding that *Otx2, Gsc, Cer-l, Hex* and *Lefty1* expression are lost in the VE of *HNF3β,Lim1* embryos indicates that the patterning of VE cells is severely affected in these embryos. In contrast, a general VE marker *Pem* is normally expressed in *HNF3β,Lim1* embryos. Therefore, some aspects of VE development occur normally in these embryos. Furthermore, histological sections, BrdU incorporation studies and TUNEL analysis of cell death performed on *HNF3β,Lim1* embryos during gastrulation do not show any evidence of massive cell death or proliferation defects in the epiblast (Fig. 3B,D; data not shown), which would be expected if the trophic function of the VE was affected in these embryos (Tam and Behringer, 1997). Altogether, these results demonstrate that the epiblast defects observed in *HNF3β,Lim1* embryos are due to loss of the patterning function of the VE.

To confirm that the patterning defects in *HNF3β,Lim1* embryos are due to the function of *HNF3β* and *Lim1* in the VE, we have generated chimeric embryos containing double mutant cells in the VE layer and a completely wild-type embryonic region. These chimeric embryos show no rescue of the *HNF3β,Lim1* phenotype, demonstrating that the abnormal patterning of the epiblast and the expanded primitive streak region observed in *HNF3β,Lim1* embryos are due to a requirement of *HNF3β* and *Lim1* functions in the VE. A direct role for these genes in extraembryonic ectoderm of chimeric embryos, which is also made of double mutant *HNF3β,Lim1* cells, can be excluded since the two genes are not expressed in this tissue. Thus, *HNF3β* and *Lim1* are required in the VE for its patterning function.

Interestingly, *HNF3β,Lim1* embryos show defects that are similar to those observed in mutant embryos for the *Smad2* gene, a transducer of TGFβ/activin signalling (Waldrip et al., 1998). Chimeric studies have also shown that the requirement for *Smad2* is in extraembryonic tissues, VE cells and/or extraembryonic ectoderm cells. *Lim1* and *HNF3β* are not expressed in the VE of $Smad2^{Robm1}$ homozygous embryos, suggesting that the $Smad2^{Robm1}$ phenotype is in part due to the lack of VE expression of *HNF3β* and *Lim1*, and that *Smad2* functions upstream of these genes. This hypothesis is tempting in light of the data obtained in *Xenopus* and zebrafish embryos, demonstrating that the homologs of these two genes are inducible by the TGFβ superfamily molecule Nodal (Toyama et al., 1995; Rebbert and Dawid, 1997; Feldman et al., 1998; Howell and Hill, 1997).

VE-derived signals pattern the epiblast of the mouse embryo

A requirement of *HNF3β* and *Lim1* in the VE for correct A-P patterning of the epiblast implies that extrinsic signals derived from the VE and dependent on *HNF3β* and *Lim1* are required to maintain the pluripotentiality of epiblast cells and/or to prevent them from adopting a primitive streak fate. Our analysis of gene expression in the VE of *HNF3β,Lim1* embryos suggests that Cer-l and Lefty1 are candidate molecules for signalling between VE and epiblast cells.

Gain-of-function as well as biochemical experiments performed in *Xenopus* embryos have demonstrated that *Cerberus* (X-cer) triggers head induction and suppresses trunk-tail mesoderm formation by inhibiting the signalling activities of Nodal, BMP4 and Wnt through direct binding to these molecules (Bouwmeester et al., 1996, Hsu et al., 1998; Piccolo et al., 1999). Although Cer-l is not able to mimic the head-inducing activity of *X-Cer* when injected ventrally in *Xenopus* embryos, it is able to inhibit BMP activity in *Xenopus* and mammalian assays (Belo et al., 1997; Biben et al., 1998; Pearce et al., 1999), as well as Nodal and X-Wnt8 activities in *Xenopus* assays (J. A. Belo and E. M. De Robertis, personal communication).

Another interesting candidate signalling molecule expressed in VE and whose expression is lost in *HNF3β,Lim1* embryos is Lefty1. In zebrafish, a novel gene called *antivin*, belonging to a new subclass of the TGFβ superfamily that also contains the mouse *Lefty1* and *Lefty2* genes, has been shown to function as an antagonist of TGFβ signalling (Thisse and Thisse, 1999). Moreover, *Lefty1* has been shown to have anti-BMP activity in *Xenopus* animal cap assays (Meno et al., 1997). In addition, a null mutation of *Lefty1* in mice demonstrates that this gene regulates the expression of *Lefty2* and *Nodal* in the lateral plate mesoderm, yet the *Lefty1* mutant embryos gastrulate normally (Meno et al., 1998). Thus, we propose that *HNF3β* and *Lim1* function in the VE to control directly or indirectly the expression of Cer-l, Lefty1 and possibly other unidentified secreted molecules. These molecules would then act in combination to block mesoderm formation in the anterior

regions of the epiblast, thus permitting the development of anterior neural structures. Consistent with a role for the anterior visceral endoderm to block mesoderm formation in the anterior epiblast, explants of the anterior epiblast isolated from the VE of wild-type embryos at 6.5 d.p.c. and cultured for 2 days show widespread expression of *T* (A. P.-G. and S.-L. A., unpublished results).

HNF3β and *Lim1* may be required in the anterior primitive streak to specify dorsal mesoderm cell fates

The function proposed above for *Lim1* and *HNF3β* in the VE would explain the abnormal patterning of the epiblast as well as the absence of ectoderm derivatives observed in *HNF3β,Lim1* embryos. However, it does not explain the absence of dorsal mesoderm and the exclusive production of extraembryonic and ventral mesoderm populations. The molecular mechanisms involved in the development of different D-V populations of mesoderm are not well understood in the mouse embryo. Analyses of *Fgfr1* and *BMP4* mutants have provided some evidence for the existence of dorsalising and ventralising signals involved in patterning mesoderm cells as they ingress through the different segments of the primitive streak (Yamaguchi et al., 1994; Deng et al., 1994; Winnier et al., 1995). It is generally thought that ventral signals such as BMP4 would be produced by extraembryonic ectoderm and later by ventral mesoderm, whereas dorsalising signals would be produced by the anterior primitive streak expressing BMP antagonists such as chordin, noggin and follistatin. Indeed ectopic graft of the node of a late streak embryo into the posterior proximal region of the epiblast induces the formation of a truncated secondary axis containing somites derived from host tissue (Beddington, 1994). Thus, a likely explanation for the absence of dorsal mesoderm derivatives in *HNF3β,Lim1* embryos is the lack of anterior primitive streak shown by the absence of *Gsc* expression. Loss of axial mesoderm would be a direct consequence of the absence of precursors cells normally located in the anterior primitive streak, whereas the absence of paraxial mesoderm would be due to the lack of dorsalising signals. The absence of anterior primitive streak cells itself could be a direct effect of the lack of expression of *HNF3β* and *Lim1* in these cells, but it could also be a consequence of the defect in VE discussed above. In *Smad2^{Robm1}* embryos, the anterior primitive streak also fails to form, suggesting that VE signals patterning the epiblast could also be required for the induction of the anterior primitive streak. To address synergistic function of these two genes in anterior primitive streak cells, we will derive *HNF3β$^{-/-}$;Lim1$^{-/-}$* ES cells in the future to generate the reverse type of chimeric embryos, whereby the VE and the embryonic region are made up entirely of wild-type and *HNF3β,Lim1* mutant cells, respectively. In addition, synergistic functions of the two genes in notochordal precursors in the anterior primitive streak are clearly required for notochord development, as *HNF3β$^{+/-}$;Lim1$^{-/-}$* embryos lack a notochord and show fusion of somites in the midline, in contrast to normal development of these two structures in *HNF3β$^{+/-}$* and *Lim1$^{-/-}$* embryos (data not shown).

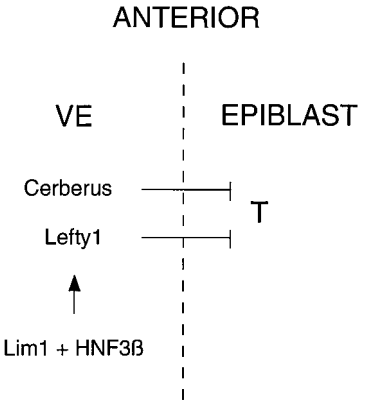

Fig. 9. Model of molecular interactions involved in restriction of *T* expression in the epiblast at the anterior end of the mouse embryo. Cer-l and Lefty1, secreted by AVE cells, inhibit *T* expression in anterior epiblast cells. Our data suggest that expression of *Cer-1* and *Lefty1* in the AVE is positively regulated, directly or indirectly, by the combined activities of the transcription factors *Lim1* and *HNF3β* in the VE.

How do *HNF3β* and *Lim1* interact in the visceral endoderm?

The present study demonstrates that *HNF3β* and *Lim1* interact in the VE to pattern the epiblast. The coexpression of the two genes in VE cells strongly suggests that the two proteins act in the same cell. An interaction at the cellular level could involve the direct regulation of a common target (e.g. *Cer-l*) or the involvement in parallel pathways leading to the same signalling event. In any case, loss of one of the two genes is not sufficient to abolish patterning of the epiblast. A role of *HNF3β* in the VE to ensure the proper elongation of the primitive streak has been previously demonstrated with chimeric embryos (Dufort et al., 1998). Although *Lim1* function in the VE has not yet been reported, *Lim1* appears to be required in the VE and the prechordal mesoderm to induce head development in chimeric embryos (W. S. and R. R. B, unpublished results). Thus these two genes have separate functions in the VE, but the double mutant analysis reveals that they also share a new and earlier function of patterning the epiblast.

In summary, we have shown that *HNF3β* and *Lim1* function synergistically in the VE before and during gastrulation to establish the A-P polarity of the embryo, by restricting the extent of epiblast territory that contributes to the primitive streak. The model that we propose invokes a role for these transcription factors in regulating the expression of secreted molecules from the VE that act on the epiblast by preventing mesoderm formation in the anterior regions of the embryo (Fig. 9).

The loss of posterior neural tissues in double mutant embryos is most likely due to additional functions of the two genes in establishment of anterior primitive streak cells that are required for trunk development. Future experiments will be aimed at testing different steps of the model proposed in Fig. 9 by coculturing epiblast isolated from wild-type embryos with cells expressing the different candidate signalling molecules.

We are grateful to Drs R. Beddington, M. Blum, P. Chambon, H. Hamada, R. Harvey, D. Henrique, B. Herrmann, B. L. Hogan, M. Kuehn, G. Martin, V. E. Papaioannou, Y. Saga, H. Scholer, F. Perrin-

Schmitt, and D. G. Wilkinson for generous gift of probes, Muriel Rhinn for help with whole-mount in situ hybridisation experiments, Valerie Meyer, Veronique Pfister and Patrice Goetz-Reiner for excellent technical assistance, Andrée Dierich and Marianne Lemeur for generating ES-morula chimeras and François Guillemot and Elizabeth Robertson for critical reading of manuscript. This work was supported by research grants from the European Community Biotech programme to S.-L. A. and from the Human Frontier Science Program and by funds from the Institute National de la Santé et de la Recherche Médicale, the Centre National de la Recherche Scientifique, the Association pour la Recherche sur le Cancer and the Hôpital Universitaire de Strasbourg.

REFERENCES

Ang, S. L., Rossant, J. (1994). HNF-3beta is essential for node and notochord formation in mouse development. *Cell* **78,** 561-574.

Ang, S. L., Conlon, R. A., Jin, O. and Rossant, J. (1994). Positive and negative signals from mesoderm regulate the expression of mouse *Otx2* in ectoderm explants. *Development* **120,** 2979-2989.

Barnes, J. D., Crosby, J. L., Jones, C. M., Wright, C. V. and Hogan, B. L. (1994). Embryonic expression of Lim-1, the mouse homolog of *Xenopus* Xlim-1, suggests a role in lateral mesoderm differentiation and neurogenesis. *Dev. Biol.* **161,** 168-178.

Beddington, R. S. P., Morgenstein, J., Land, H. and Hogan, A. (1989). An situ transgenic enzyme marker for the midgestation mouse embryo and the visualization of the inner cell mass clones during early organogenesis. *Development* **106,** 37-46.

Beddington, R. S. P. (1994). Induction of a second neural axis by the mouse node. *Development* **120,** 613-620.

Beddington, R. S. and Robertson, E. J. (1998). Anterior patterning in mouse. *Trends Genet.* **14,** 277-284.

Beddington, R. S. and Robertson, E. J. (1999). Axis development and early asymmetry in mammals. *Cell* **96,** 195-209.

Belo, J. A., Bouwmeester, T., Leyns, L., Kertesz, N., Gallo, M., Follettie, M. and De Robertis, E. M. (1997). Cerberus-like is a secreted factor with neutralizing activity expressed in the anterior primitive endoderm of the mouse gastrula. *Mech. Dev.* **68,** 45-57.

Bettenhausen, B., Hrabe de Angelis, M., Simon, D., Guenet, J. L. and Gossler, A. (1995). Transient and restricted expression during mouse embryogenesis of *Dll1*, a murine gene closely related to Drosophila Delta. *Development* **121,** 2407-2418.

Biben, C., Stanley, E., Fabri, L., Kotecha, S., Rhinn, M., Drinkwater, C., Lah, M., Wang, C. C., Nash, A., Hilton, D., Ang, S. L., Mohun, T. and Harvey, R. P. (1998). Murine cerberus homologue mCer-1: a candidate anterior patterning molecule. *Dev. Biol.* **194,** 135-151.

Blum, M., Gaunt, S. J., Cho, K. W., Steinbeisser, H., Blumberg, B., Bittner, D. and De Robertis, E. M. (1992). Gastrulation in the mouse: the role of the homeobox gene *goosecoid*. *Cell* **69,** 1097-1106.

Bouwmeester, T., Kim, S., Sasai, Y., Lu, B. and De Robertis, E. M. (1996). Cerberus is a head-inducing secreted factor expressed in the anterior endoderm of Spemann's organizer. *Nature* **382,** 595-601.

Chapman, D. L., Agulnik, I., Hancock, S., Silver, L. M. and Papaioannou, V. E. (1996). *Tbx6*, a mouse T-Box gene implicated in paraxial mesoderm formation at gastrulation. *Dev. Biol.* **180,** 534-542.

Collignon, J., Sockanathan, S., Hacker, A., Cohen-Tannoudji, M., Norris, D., Rastan, S., Stevanovic, M., Goodfellow, P. N. and Lovell-Badge, R. (1996). A comparison of properties of *Sox-3* with *Sry* and two related genes, Sox-1 and Sox-2. *Development* **122,** 509-520.

Conlon, R. A. and Herrmann, B. G. (1993). Detection of messenger RNA by in situ hybridization to postimplantation embryo whole mounts. *Methods Enzymol.* **225,** 373-383.

Crossley, P. H. and Martin, G. R. (1995). The mouse *Fgf8* gene encodes a family of polypeptides and is expressed in regions that direct outgrowth and patterning in the developing embryo. *Development* **121**, 439-451.

Davis, C. A., Holmyard, D. P., Millen, K. J. and Joyner, A. L. (1991). Examining pattern formation in mouse, chicken and frog embryos with an En-specific antiserum. *Development* **111,** 287-298.

Deng, C. X., Wynshaw-Boris, A., Shen, M. M., Daugherty, C., Ornitz, D. M. and Leder, P. (1994). Murine FGFR-1 is required for early postimplantation growth and axial organization. *Genes Dev.* **8,** 3045-3057.

Downs, K. M. and Davies, T. (1993). Staging of gastrulating mouse embryos by morphological landmarks in the dissecting microscope. *Development* **118,** 1255-1266.

Dufort, D., Schwartz, L., Harpal, K. and Rossant, J. (1998). The transcription factor HNF3beta is required in visceral endoderm for normal primitive streak morphogenesis. *Development* **125,** 3015-3025.

Feldman, B., Gates, M. A., Egan, E. S., Dougan, S. T., Rennebeck, G., Sirotkin, H. I., Schier, A. F. and Talbot, W. S. (1998). Zebrafish organizer development and germ-layer formation require nodal-related signals. *Nature* **395,** 181-185.

Filosa, S., Rivera-Perez, J. A., Perea-Gomez, A., Gansmuller, A., Sasaki, H., Behringer, R. R. and Ang, S. L. (1997). *Goosecoid* and *HNF-3beta* genetically interact to regulate neural tube patterning during mouse embryogenesis. *Development* **124,** 2843-2854.

Gradwohl, G., Fode, C. and Guillemot, F. (1996). Restricted expression of a novel bHLH atonal-related protein to undifferentiated neural progenitors. *Dev. Biol.* **180,** 227-241.

Hogan, B., Beddington, R., Constantini, F. and Lacy, E. (1994). *Manipulating the Mouse Embryo: A Laboratory Manual*. New York: Cold Spring Harbor.

Howell, M. and Hill, C. S. (1997). XSmad2 directly activates the activin-inducible, dorsal mesoderm gene XFKH1 in Xenopus embryos. *EMBO J.* **16,** 7411-7421.

Hsu, D. R., Economides, A. N., Wang, X., Eimon, P. M. and Harland, R. M. (1998). The Xenopus dorsalizing factor Gremlin identifies a novel family of secreted proteins that antagonize BMP activities. *Mol. Cell.* **1,** 673-683.

Laird, P. W., Zijderveld, A., Linders, K., Rudnicki, M. A., Jaenisch, R. and Berns, A. (1991). Simplified mammalian DNA isolation procedure. *Nucleic Acids Res.* **19,** 4293.

Lawson, K. A., Meneses, J. J. and Pedersen, R. A. (1991). Clonal analysis of epiblast fate during germ layer formation in the mouse embryo. *Development* **113,** 891-911.

Lemaire, P. and Kodjabachian, L. (1996). The vertebrate organizer: structure and molecules. *Trends Genet.* **12,** 525-531.

Lin, T. P., Labosky, P. A., Grabel, L. B., Kozak, C. A., Pitman, J. L., Kleeman, J. and MacLeod, C. L. (1994). The Pem homeobox gene is X-linked and exclusively expressed in extraembryonic tissues during early murine development. *Dev. Biol.* **166,** 170-179.

Meno, C., Saijoh, Y., Fuji, H., Ikeda, M., Yokoyama, T., Yokoyama, M., Toyoda, Y. and Hamada, H. (1996). Left-right asymmetric expression of the TGF beta-family member lefty in mouse embryos. *Nature* **381,** 151-155.

Meno, C., Ito, Y., Saijoh, Y., Matsuda, Y., Tashiro, K., Kuhara, S. and Hamada, H. (1997). Two closely-related left-right asymmetrically expressed genes, lefty-1 and *lefty-2*: their distinct expression domains, chromosomal linkage and direct neuralizing activity in *Xenopus* embryos. *Genes Cells* **2,** 513-524.

Meno, C., Shimono, A., Saijoh, Y., Yashiro, K., Mochida, K., Ohishi, S., Noji, S., Kondoh, H. and Hamada, H. (1998). lefty-1 is required for left-right determination as a regulator of lefty-2 and Nodal. *Cell* **94,** 287-297.

Moens, C. B., Auerbach, A. B., Conlon, R. A., Joyner, A. L. and Rossant, J. A. (1992). Targeted mutation reveals a role for N-myc in branching morphogenesis in the embryonic mouse lung. *Genes Dev.* **6,** 691-704.

Oulad-Abdelghani, M., Chazaud, C., Bouillet, P., Mattei, M. G., Dolle, P. and Chambon, P. (1998). Stra3/lefty, a retinoic acid-inducible novel member of the transforming growth factor-beta superfamily. *Int J Dev Biol.* **42,** 23-32.

Pearce, J. J., Penny, G. and Rossant, J. (1999). A mouse cerberus/Dan-related gene family. *Dev. Biol.* **209,** 98-110.

Piccolo, S., Agius, E., Leyns, L., Bhattacharyya, S., Grunz, H., Bouwmeester, T. and De Robertis, E. M. (1999). The head inducer Cerberus is a multifunctional antagonist of Nodal, BMP and Wnt signals. *Nature* **397,** 707-710.

Rebbert, M. L. and Dawid, I. B. (1997). Transcriptional regulation of the Xlim-1 gene by activin is mediated by an element in intron I. *Proc. Natl Acad. Sci. USA.* **94,** 9717-9722.

Rhinn, M., Dierich, A., Shawlot, W., Behringer, R. R., Le Meur, M. and Ang, S. L. (1998). Sequential roles for *Otx2* in visceral endoderm and neuroectoderm for forebrain and midbrain induction and specification. *Development* **125,** 845-856.

Rivera-Perez, J. A., Mallo, M., Gendron-Maguire, M., Gridley, T. and Behringer, R. R. (1995). *Goosecoid* is not an essential component of the mouse gastrula organizer but is required for craniofacial and rib development. *Development* **121,** 3005-3012.

Rosner, M. H., Vigano, M. A., Ozato, K., Timmons, P. M., Poirier, F., Rigby, P. W. and Staudt, L. M. (1990). A POU-domain transcription factor in early stem cells and germ cells of the mammalian embryo. *Nature* **345,** 686-692.

Saga, Y., Hata, N., Kobayashi, S., Magnuson, T., Seldin, M. F. andTaketo, M. M. (1996). MesP1: a novel basic helix-loop-helix protein expressed in the nascent mesodermal cells during mouse gastrulation. *Development* **122,** 2769-2778.

Shawlot, W. and Behringer, R. R. (1995). Requirement for Lim1 in head-organizer function. *Nature* **374,** 425-430.

Simeone, A. (1998). Otx1 and Otx2 in the development and evolution of the mammalian brain. *EMBO J.* **17,** 6790-6798.

Tam, P. P. and Behringer, R. R. (1997). Mouse gastrulation: the formation of a mammalian body plan. *Mech. Dev*. **68,** 3-25.

Thisse, C. and Thisse, B. (1999). Antivin, a novel and divergent member of the TGFbeta superfamily, negatively regulates mesoderm induction. *Development* **126,** 229-240.

Thomas, P. and Beddington, R. S. P. (1996). Anterior primitive endoderm may be responsible for patterning the anterior neural plate in the mouse embryo. *Curr. Biol.* **6,** 1487-1496.

Thomas, P. Q., Brown, A. and Beddington, R. S. (1998). Hex: a homeobox gene revealing peri-implantation asymmetry in the mouse embryo and an early transient marker of endothelial cell precursors. *Development* **125,** 85-94.

Toyama, R., O'Connell, M. L., Wright, C. V., Kuehn, M. R. and Dawid, I. B. (1995). Nodal induces ectopic *goosecoid* and *lim1* expression and axis duplication in zebrafish. *Development* **121,** 383-391.

Varlet, I., Collignon, J., Robertson, E. J. (1997). Nodal expression in the primitive endoderm is required for specification of the anterior axis during mouse gastrulation. *Development* **124,** 1033-1044.

Waldrip, W. R., Bikoff, E. K., Hoodless, P. A., Wrana, J. L. and Robertson, E. J. (1998). Smad2 signaling in extraembryonic tissues determines anterior-posterior polarity of the early mouse embryo. *Cell* **92,** 797-808.

Weinstein, D. C., Ruiz i Altaba, A., Chen, W. S., Hoodless, P., Prezioso, V. R., Jessell, T.M. and Darnell, J. E. (1994). The winged-helix transcription factor HNF-3beta is required for notochord development in the mouse embryo. *Cell* **78,** 575-588.

Wilkinson, D. G., Bhatt, S. and McMahon, A. P. (1989). Expression pattern of the FGF-related proto-oncogene int-2 suggests multiple roles in fetal development. *Development* **105,** 131-136.

Wilkinson, D. G., Bhatt, S. and Herrmann, B. G. (1990). Expression pattern of the mouse *T* gene and its role in mesoderm formation. *Nature* **343,** 657-659.

Winnier, G., Blessing, M., Labosky, P. A. and Hogan, B. L. (1995). Bone morphogenetic protein-4 is required for mesoderm formation and patterning in the mouse. *Genes Dev.* **9,** 2105-2116.

Wolf, C., Thisse, C., Stoetzel, C., Thisse, B., Gerlinger, P. and Perrin-Schmitt, F. (1991). The M-twist gene of Mus is expressed in subsets of mesodermal cells and is closely related to the *Xenopus* X-twi and the Drosophila twist genes. *Dev. Biol*. **143,** 363-373.

Yamada, G., Mansouri, A., Torres, M., Stuart, E. T., Blum, M., Schultz, M., De Robertis, E. M. and Gruss, P. (1995). Targeted mutation of the murine *goosecoid* gene results in craniofacial defects and neonatal death. *Development* **121,** 2917-2922.

Yamaguchi, T. P., Dumont, D. J., Conlon, R. A., Breitman, M. L. and Rossant, J. (1993). flk-1, an flt-related receptor tyrosine kinase is an early marker for endothelial cell precursors. *Development* **118,** 489-498.

Yamaguchi, T. P., Harpal, K., Henkemeyer, M. and Rossant, J. (1994). fgfr-1 is required for embryonic growth and mesodermal patterning during mouse gastrulation. *Genes Dev.* **8,** 3032-3044.